NATIONAL ADVISORY COMMITTEE FOR AERONAUTICS

TECHNICAL NOTE 2284

LIFT, PITCHING MOMENT, AND SPAN LOAD CHARACTERISTICS OF WINGS AT LOW SPEED AS AFFECTED BY VARIATIONS OF SWEEP AND ASPECT RATIO

By Edward J. Hopkins

Ames Aeronautical Laboratory
Moffett Field, Calif.

NACA

Washington
January 1951

NATIONAL ADVISORY COMMITTEE FOR AERONAUTICS

TECHNICAL NOTE 2284

LIFT, PITCHING MOMENT, AND SPAN LOAD CHARACTERISTICS OF WINGS AT LOW SPEED AS AFFECTED BY VARIATIONS OF SWEEP AND ASPECT RATIO

By Edward J. Hopkins

SUMMARY

Measurements of the lift, pitching moment, and pressure distribution of a wing which was swept -40°, -30°, 0°, 35°, and 45° were made at low speed in a wind tunnel. The wing span was decreased to give aspect ratios of 6.8, 5.3, 4.2, 3.4, and 2.8 with corresponding taper ratios of approximately 0.4 to 0.7. The experimental effects of independent variations of sweep and aspect ratio on the lift-curve slopes, the span load distributions, the aerodynamic-center locations, and the spanwise center-of-pressure locations are compared with the effects estimated by use of the Weissinger method.

A sufficient reduction of the aspect ratio of the swept wings eliminated the static longitudinal instability at the moderate to high lift coefficients, but failed to eliminate the premature local stalling associated with swept wings. The Weissinger method gave good agreement with the experimental lift-curve slopes, but slightly underestimated the lift carried over the outer portions of the wings.

INTRODUCTION

In recent years considerable attention has been given swept wings because of the benefits to be derived from sweep at high speeds. Although large amounts of sweep may lead to plan forms capable of efficient flight at high speeds, sweep causes numerous stability and control problems. An investigation was undertaken to explore the primary changes in the low-speed lift, pitching-moment, and span load characteristics of wings caused by independent variations of sweep and aspect ratio. This report summarizes the experimental results obtained in one of the Ames 7- by 10-foot wind tunnels for various plan forms.

Several theoretical methods for estimating the span load and the lift characteristics of wings have been studied from the standpoint of accuracy and time of application (reference 1). As a result of this study, the Weissinger method appeared best suited and was used for the theoretical investigation of the numerous plan forms in reference 2. The results from applying this method to the wings of the present investigation are presented and compared with the experimental results.

NOTATION

A aspect ratio $\left(\frac{b^2}{S}\right)$

b wing span measured perpendicular to the air stream, feet

c wing chord measured parallel to the air stream, feet

c' wing chord measured perpendicular to the sweep reference line, feet

$\bar{c}$ mean aerodynamic chord, $\left(\frac{\int_0^{0.5b} c^2\,dy}{\int_0^{0.5b} c\,dy}\right)$, feet

c_{av} average chord $\left(\frac{S}{b}\right)$, feet

c_R root chord, feet

c_T tip chord, feet

C_L lift coefficient $\left(\frac{L}{qS}\right)$

ΔC_L additional-total-lift coefficient, change of total-lift coefficient produced by a unit change of angle of attack within the linear range of the lift curve

$C_{L_{max}}$ maximum lift coefficient

C_{L_α} lift-curve slope (measured through $\alpha = 0^\circ$), per degree

ΔC_l additional-local-lift coefficient, change of local-lift coefficient produced by a unit change of angle of attack within the linear range of the lift curve

C_m pitching-moment coefficient $\left(\frac{M}{qS\bar{c}}\right)$

K_1 correction constant for angle of attack

K_2 correction constant for lift coefficient

K_3 correction constant for pitching-moment coefficient

L wing lift, pounds

M wing pitching moment about the lateral axis through the 25-percent point of the mean aerodynamic chord, foot-pounds

q free-stream dynamic pressure, pounds per square foot

R Reynolds number $\left(\frac{V\bar{c}}{\nu}\right)$

S wing area, square feet

V free-stream velocity, feet per second

y lateral distance measured from reflection plane, feet

α angle of attack, degrees

$\alpha_{C_{L_{max}}}$ angle of attack at maximum lift coefficient, degrees

λ taper ratio $\left(\frac{c_T}{c_R}\right)$

Λ angle of sweep of the line joining the quarter-chord points of the NACA 64_1-212 sections which were perpendicular to this line, positive for sweepback, degrees

ν kinematic viscosity, feet squared per second

Subscript

u uncorrected

CORRECTIONS

The experimental data were corrected for the effects of the wind-tunnel walls by the method of reference 3. The corrections applied to the data for the swept wings were the same as for unswept wings of the same aspect ratio, taper ratio, and area. A few previous checks of corrections for similar plan forms had indicated that a negligible error was involved in applying the corrections in this manner. The angles of attack and the lift and pitching-moment coefficients were corrected as follows:

$$\alpha = \alpha_u + K_1 C_{L_u}$$

$$C_L = C_{L_u} + K_2 C_{L_u}$$

$$C_m = C_{m_u} + K_3 C_{L_u}$$

where K_1, K_2, and K_3 are constants to be found in table I and the subscript u denotes the uncorrected values.

DESCRIPTION OF MODEL

The model wings used in this investigation were mounted in one of the Ames 7- by 10-foot wind tunnels on a turntable flush with the tunnel floor which served as a reflection plane corresponding to the plane of symmetry (fig. 1). The variations of the sweep angle were accomplished by rotating the semispan model wings about a point at 38 percent of the root chord of the unswept wing. The aspect ratio was varied by a progressive reduction in wing span. The geometry of each of the wing plan forms, including an illustration of the geometric construction of a typical tip plan form, is shown in figure 2. The unswept wings had the NACA 64_1-212 section perpendicular to the quarter-chord line. For the swept wings, the angle between the NACA 64_1-212 section and the plane of symmetry was equal to the angle of sweep. The spanwise locations of the rows of pressure orifices in the model are shown in figure 3.

TESTS

The data presented herein were obtained at a dynamic pressure of 40 pounds per square foot. The corresponding Reynolds number for each plan form is given in table II. It should be noted that, because of the manner in which the plan forms of the wings were obtained, the wing chords parallel to the plane of symmetry (for wings of constant aspect ratio) became slightly larger with increase in sweep angle which resulted in an increase of streamwise Reynolds number.

In order to ascertain whether these changes of Reynolds number with sweep angle (table II) affected the lift and pitching-moment coefficients, several of the swept wings were tested throughout a range of Reynolds numbers from 1.2 million to 2.2 million. This range brackets the range of Reynolds numbers that resulted from testing all the wings at a constant dynamic pressure. Only insignificant effects of scale on the aerodynamic characteristics were found in this range.

PRESENTATION OF RESULTS

The lift and pitching-moment characteristics of the various model wings are presented in figures 4(a) to 4(e). Summarized in figure 5 are the effects of variations of sweep and of aspect ratio on the lift-curve slopes, on the angles of attack for maximum lift coefficient, on the maximum lift coefficients, and on the longitudinal-stability characteristics. The predicted lift-curve slopes from reference 2 (the Weissinger method) are also presented in figure 5. Effects of the sweep and aspect-ratio variations on the aerodynamic-center locations from the present experiments and from calculations by the method of reference 2 are presented in figure 6. The experimental aerodynamic-center locations were determined from the slopes of the pitching-moment curves for the various plan forms measured through zero lift coefficient (figs. 4(a) to 4(e)).

The spanwise variations of $\Delta c_l/\Delta C_L$ and of $\Delta c_l c/\Delta C_L c_{av}$ obtained from the experiments and from reference 2 are presented in figures 7 and 8. The effects of sweep and aspect-ratio variations on the spanwise center-of-pressure locations determined by use of the experimental loading curves and from reference 2 are presented in figure 9.

DISCUSSION OF RESULTS

It should be mentioned that, because of the manner in which the various plan forms were developed, each change of sweep or aspect ratio was accompanied by a change of taper ratio. The taper ratios ranged from 0.412 to 0.725. The effect on the air flow of the raked wing tips on the swept wings is unknown but is believed to have been localized near the wing tips. Some discretion should be used, therefore, in comparing some of the effects of variations of sweep and aspect ratio with the effects indicated by other investigations.

Lift and Pitching-Moment Characteristics

For all aspect ratios, either sweepforward or sweepback decreased the lift-curve slope, increased the angle of attack for maximum lift coefficient, and, in general, increased the maximum lift coefficient of the wings (fig. 5). Other swept wings at Reynolds numbers less than 2.0 million have also been observed to have greater maximum lift coefficients than unswept wings of the same aspect ratios. Insufficient evidence is available to determine the reason for this effect of sweep which may occur only at low Reynolds numbers.

It should be noted that sweep produced longitudinal instability at moderate to high lift coefficients for wings of aspect ratios 6.8 and

5.3 (figs. 4(a) and 4(b)). The lift coefficient at which this longitudinal instability first occurred decreased as the wing was swept either forward or back. However, reducing the aspect ratio of the swept wings had the effect of eliminating the longitudinal instability at the moderate to high lift coefficients, as shown in figures 4(a) to 4(e).

In an effort to determine the causes for the changes in the longitudinal stability, studies were made of the air flow in the boundary layer by means of short tufts of thread placed on the upper surface of the models. These studies indicated that a complete breakdown of flow (stall) occurred initially near the wing tips of all the swept-back models and near the wing roots of all the swept-forward models and approximately at the midsemispan of the unswept models. Reduction of the aspect ratio of the swept wings failed to eliminate these stalled areas. The improvement in the longitudinal-stability characteristics of the swept wings caused by a sufficient reduction in aspect ratio is probably mainly attributable, therefore, to the proximity of the local normal forces acting over the stalled areas to the lateral axis rather than an improvement in the air flow over the wings.

As shown by the close agreement between the experimental and theoretical lift-curve slopes (fig. 5), the Weissinger method predicted with good accuracy the lift-curve slopes of all the wings. The increase with sweep of the angle of attack for maximum lift coefficient was less for the wings having the smaller aspect ratios. The increase of the maximum lift coefficient with sweep was relatively unaffected by changes in the aspect ratio of the wings. The fact that the stability at the higher lift coefficients was primarily a function of the combination of aspect ratio and sweep, mentioned hereinbefore, was also indicated in reference 4. The combinations of aspect ratio and sweep for marginal stability at the higher lift coefficients, as determined in reference 4, are indicated by the broad curve in the plot of aspect ratio versus sweepback of figure 5. Combinations above this curve were unstable at the higher lift coefficients while those below the curve were stable. The data of the present report as indicated by the experimental points are shown to be in close agreement with the results of reference 4. It is noteworthy that the combinations of aspect ratio and sweep for marginal stability for swept-back wings from reference 4 are also valid for the swept-forward wings. The data for the swept-forward wings are indicated by the flagged symbols in figure 5.

For all aspect ratios, the experimental aerodynamic-center location relative to the mean aerodynamic chord was shifted rearward by either sweepforward or sweepback (fig. 6). In the theoretical method of reference 2, it was suggested that the aerodynamic-center location could be calculated theoretically by assuming the load to act at 25 percent of a chord (parallel to the air stream) with a spanwise location corresponding to the center of the span load as given by the Weissinger method. The results of following that procedure (shown in fig. 6) do not give good agreement with the experimental effects of sweep on the aerodynamic-center location. An improvement in the prediction of the effects of sweep on the aerodynamic-center location was accomplished by assuming the chordwise location of the center of load to be 25 percent of a chord normal to the sweep reference line rather than of a chord in the streamwise direction. (See fig. 6.) It seems reasonable to believe that better correlation with the experimental aerodynamic-center location would result by following the latter procedure because chordwise pressure-distribution measurements indicated that the chordwise center of additional local lift was close to the 25-percent point of the chord normal to the sweep reference line over the center portion of the wing span for several of the swept wings. The assumed position of the load for the improved prediction is shown below:

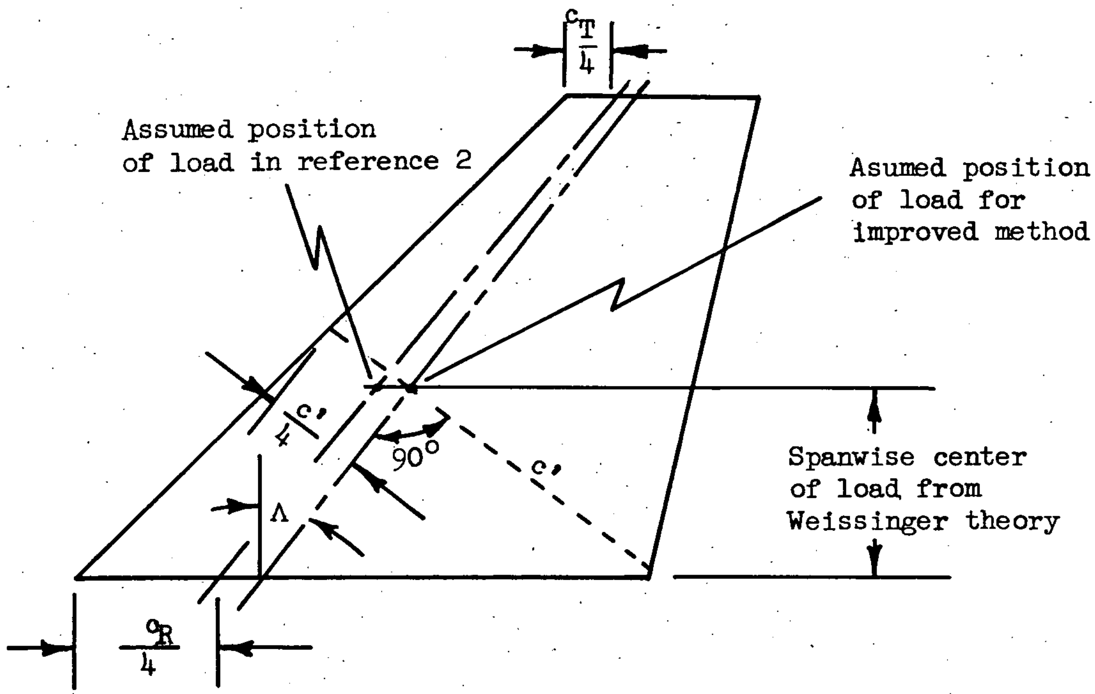

It should be observed that the measured location of the aerodynamic center for all the unswept wings was somewhat forward of the 25-percent point of the mean aerodynamic chord.

Span Load Characteristics

For all aspect ratios, a greater portion of the lift was carried near the tips of the swept-back wings and near the roots of the swept-forward wings than on the corresponding unswept wings (figs. 8(a) to 8(e)). Increasing the aspect ratio of the wings resulted in an increase of the lift near the wing tips with a corresponding reduction in lift near the wing root (figs. 7(a) to 7(e)). A comparison between the experimental and theoretical span-load characteristics (figs. 8(a) to 8(e)) indicates that, in general, the Weissinger method (reference 2) slightly underestimated the amount of lift carried on the outer portions of the wings.

Increasing the aspect ratio from 3.4 to 6.8 had a small effect on the variation of the location of the spanwise center of pressure with sweep (fig. 9). Although the experimental values of the spanwise center-of-pressure location were 1 to 2 percent of the wing semispan farther out along the semispan than the theoretical locations, the Weissinger method gave a good estimate of the variation of spanwise location of the center of pressure with sweep.

CONCLUSIONS

From the results of a wind-tunnel investigation of the effects of independent variations of sweep and of aspect ratio on the lift, pitching-moment, and span-load characteristics of wings at low speed it can be concluded that:

1. A sufficient reduction of the aspect ratio of the swept wings eliminated the longitudinal instability that occurred at moderate to high lift coefficients, but failed to eliminate the stalled areas which occurred initially near the tips of the swept-back wings and near the roots of the swept-forward wings.

2. The increase with sweep of the angle of attack for maximum lift coefficient was less for the wings with the smaller aspect ratios.

3. For all aspect ratios, an increase in sweepback or sweepforward resulted in a rearward movement of the aerodynamic center relative to the mean aerodynamic chord.

4. For all aspect ratios, a greater portion of the lift was carried near the tips of the swept-back wings and near the roots of the swept-forward wings than on the corresponding unswept wings.

5. Weissinger's theory gave good agreement with the experimental lift-curve slopes and the rate of change of spanwise center-of-pressure location with sweep, although the method slightly underestimated the lift carried over the outer portions of the wings. Improved correlation with the experimentally determined effects of sweep on the aerodynamic-center location was obtained by assuming the chordwise location of the center of span load given by the Weissinger theory to be at 25 percent of the chord normal to the sweep reference line rather than at 25 percent of the chord parallel to the air stream.

Ames Aeronautical Laboratory,
National Advisory Committee for Aeronautics,
Moffett Field, Calif., Nov. 17, 1950.

REFERENCES

1. Van Dorn, Nicholas H., and DeYoung, John: A Comparison of Three Theoretical Methods of Calculating Span Load Distribution on Swept Wings. NACA TN 1476, 1947.

2. DeYoung, John, and Harper, Charles W.: Theoretical Symmetric Span Loading at Subsonic Speeds for Wings Having Arbitrary Plan Form. NACA Rep. 921, 1948.

3. Swanson, Robert S., and Toll, Thomas A.: Jet-Boundary Corrections for Reflection-Plane Models in Rectangular Wind Tunnels. NACA Rep. 770, 1943.

4. Shortal, Joseph A., and Maggin, Bernard: Effect of Sweepback and Aspect Ratio on Longitudinal Stability Characteristics of Wings at Low Speeds. NACA TN 1093, 1946.

TABLE I

CONSTANTS FOR WIND-TUNNEL-WALL CORRECTIONS

(a) Constant K_1 for Correction to Angle of Attack

$$[\alpha = \alpha_u + K_1 C_{L_u}]$$

Aspect ratio	Angle of Sweep				
	45°	35°	0°	−30°	−40°
2.8	0.338	---	---	---	0.396
3.4	.403	0.346	0.275	0.383	.458
4.2	.467	.404	.357	.442	.519
5.3	.527	.469	.415	.507	.581
6.8	---	.529	.481	.570	---

(b) Constant K_2 for Correction to Lift Coefficient

$$[C_L = C_{L_u} + K_2 C_{L_u}]$$

Aspect ratio	Angle of Sweep				
	45°	35°	0°	−30°	−40°
2.8	−0.0017	---	---	---	−0.0020
3.4	−.0019	−0.0016	−0.0012	−0.0018	−.0022
4.2	−.0021	−.0019	−.0017	−.0022	−.0026
5.3	−.0026	−.0024	−.0020	−.0026	−.0030
6.8	---	−.0027	−.0025	−.0030	---

(c) Constant K_3 for Correction to Pitching-Moment Coefficient

$$[C_m = C_{m_u} + K_3 C_{L_u}]$$

Aspect ratio	Angle of Sweep				
	45°	35°	0°	−30°	−40°
2.8	0.000872	---	---	---	0.00104
3.4	.00098	0.00077	0.00054	0.00086	.00114
4.2	.00106	.00085	.00070	.00095	.00121
5.3	.00113	.00093	.00075	.00104	.00128
6.8	---	.00098	.00081	.00108	---

NACA

TABLE II

REYNOLDS NUMBERS[1] FOR TESTS OF THE VARIOUS WINGS

Angle of sweep (deg)	Aspect Ratio				
	6.8	5.3	4.2	3.4	2.8
-40	---	1.89×10^6	1.99×10^6	2.07×10^6	2.15×10^6
-30	1.64×10^6	1.72	1.80	1.90	---
0	1.43	1.49	1.56	1.49	---
35	1.59	1.67	1.75	1.82	---
45	---	1.81	1.90	1.99	2.07

[1]The Reynolds numbers are for the test dynamic pressure of 40 pounds per square foot and are based on the mean aerodynamic chords of the various wings.

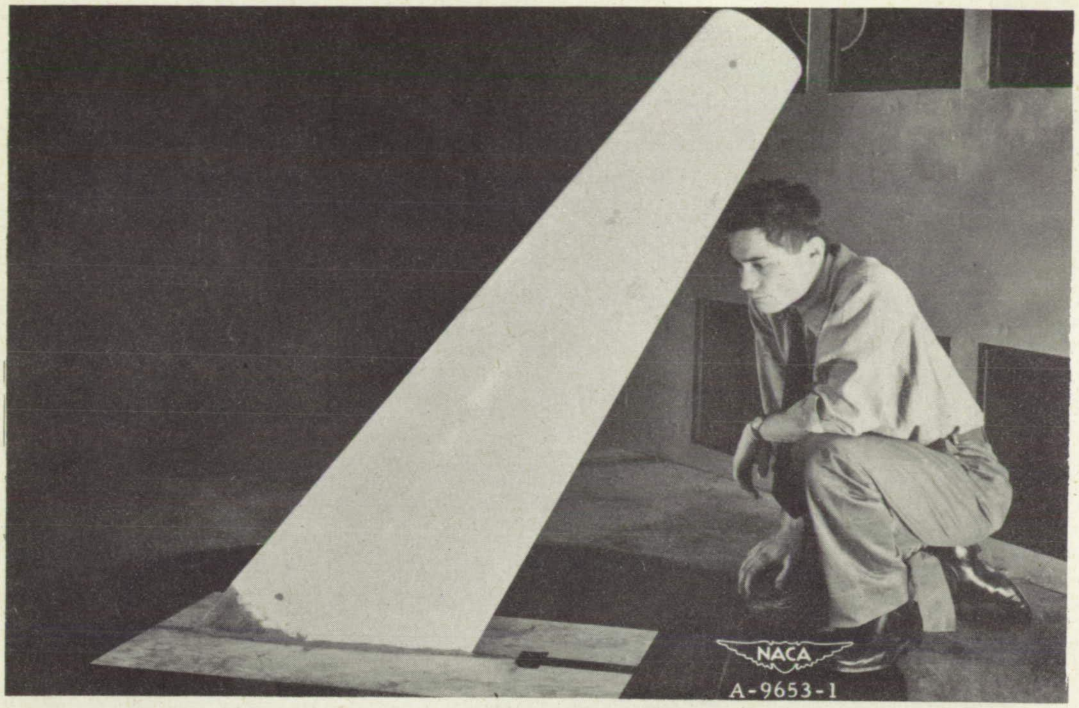

(a) 35° of sweepback.

(b) 30° of sweepforward.

Figure 1.– Swept wings of aspect ratio 6.8 mounted in one of the Ames 7– by 10–foot wind tunnels.

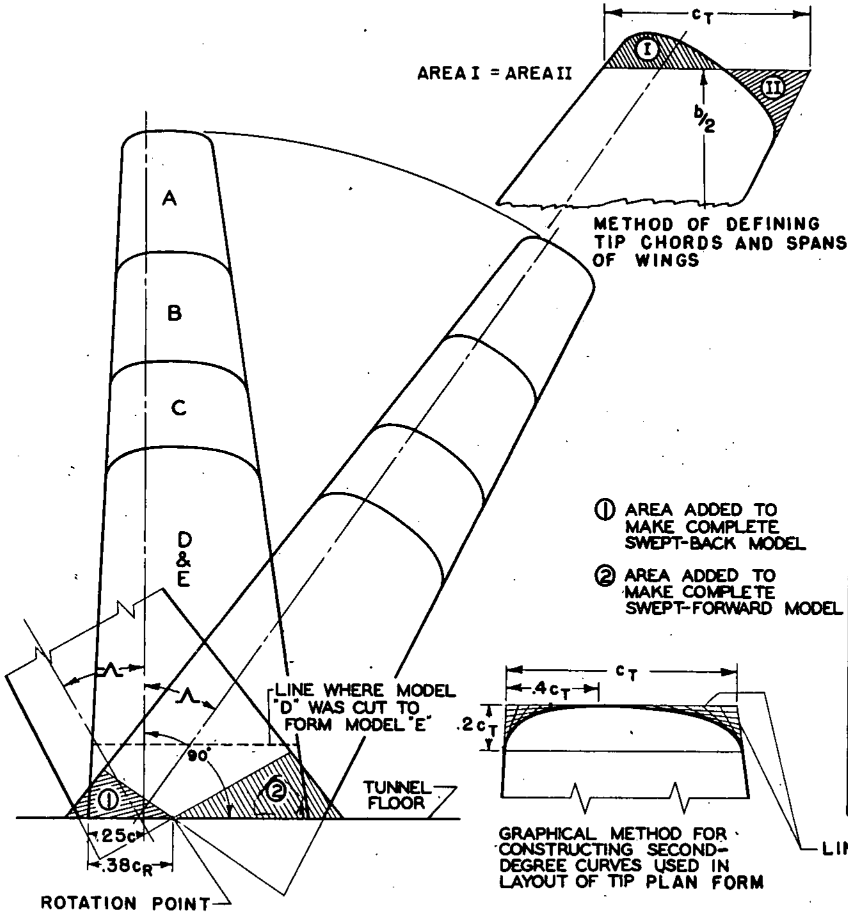

APPROX. ASPECT RATIO	MODEL	SWEEP, Λ, DEG	SEMI-SPAN $b/2$, FT	SEMI-AREA $S/2$, FT^2	ACTUAL ASPECT RATIO	TIP CHORD, FT	ROOT CHORD, FT	TAPER RATIO, λ	MEAN AERODYNAMIC CHORD, FT
6.8	A	-30	4.39	5.73	6.73	0.837	1.907	0.439	1.421
do	B	0	4.12	4.90	6.93	0.802	1.587	0.505	1.237
do	A	+35	4.25	5.36	6.74	0.770	1.843	0.418	1.380
5.3	A	-40	3.92	5.82	5.28	0.902	2.190	0.412	1.635
do	B	-30	3.68	5.09	5.32	0.985	1.907	0.516	1.494
do	C	0	3.33	4.22	5.25	0.949	1.587	0.598	1.295
do	B	+35	3.54	4.73	5.30	0.962	1.843	0.522	1.449
do	A	+45	3.75	5.26	5.35	0.880	2.088	0.421	1.566
4.2	B	-40	3.32	5.20	4.24	1.150	2.190	0.525	1.724
do	C	-30	3.04	4.36	4.24	1.147	1.907	0.601	1.559
do	D	0	2.71	3.56	4.13	1.078	1.587	0.679	1.349
do	C	+35	2.91	4.04	4.19	1.119	1.843	0.607	1.516
do	B	+45	3.14	4.64	4.25	1.116	2.088	0.534	1.651
3.4	C	-40	2.76	4.46	3.42	1.381	2.190	0.630	1.795
do	D	-30	2.53	3.74	3.42	1.359	1.907	0.712	1.648
do	E	0	2.17	2.73	3.45	1.078	1.487	0.725	1.294
do	D	+35	2.40	3.39	3.40	1.281	1.843	0.695	1.579
do	C	+45	2.59	3.96	3.39	1.300	2.088	0.622	1.725
2.8	D	-40	2.34	3.84	2.85	1.500	2.190	0.685	1.867
do	D	+45	2.16	3.31	2.82	1.466	2.088	0.702	1.795

FIGURE 2. – MODEL GEOMETRY.

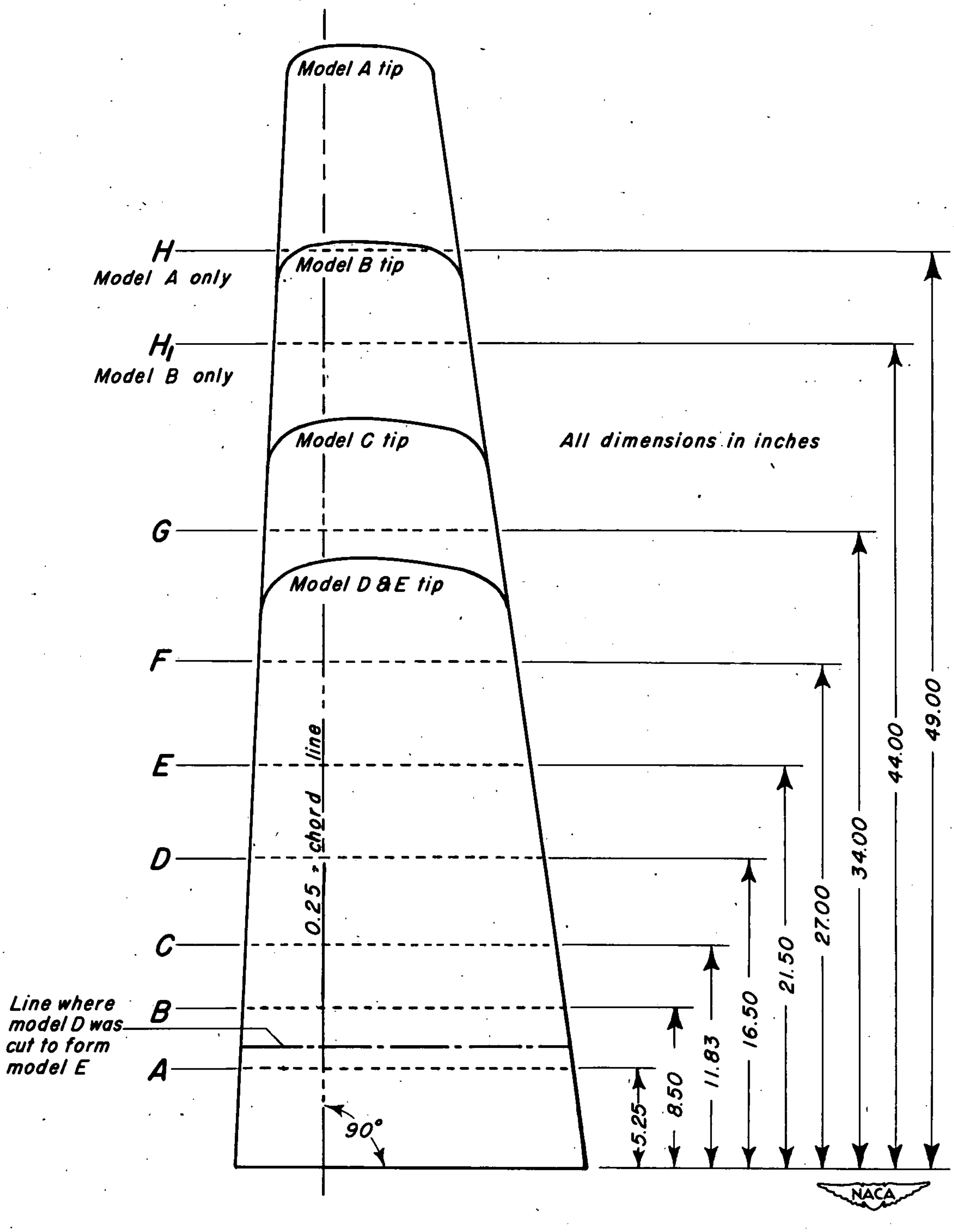

Figure 3.– Spanwise position of pressure tubes.

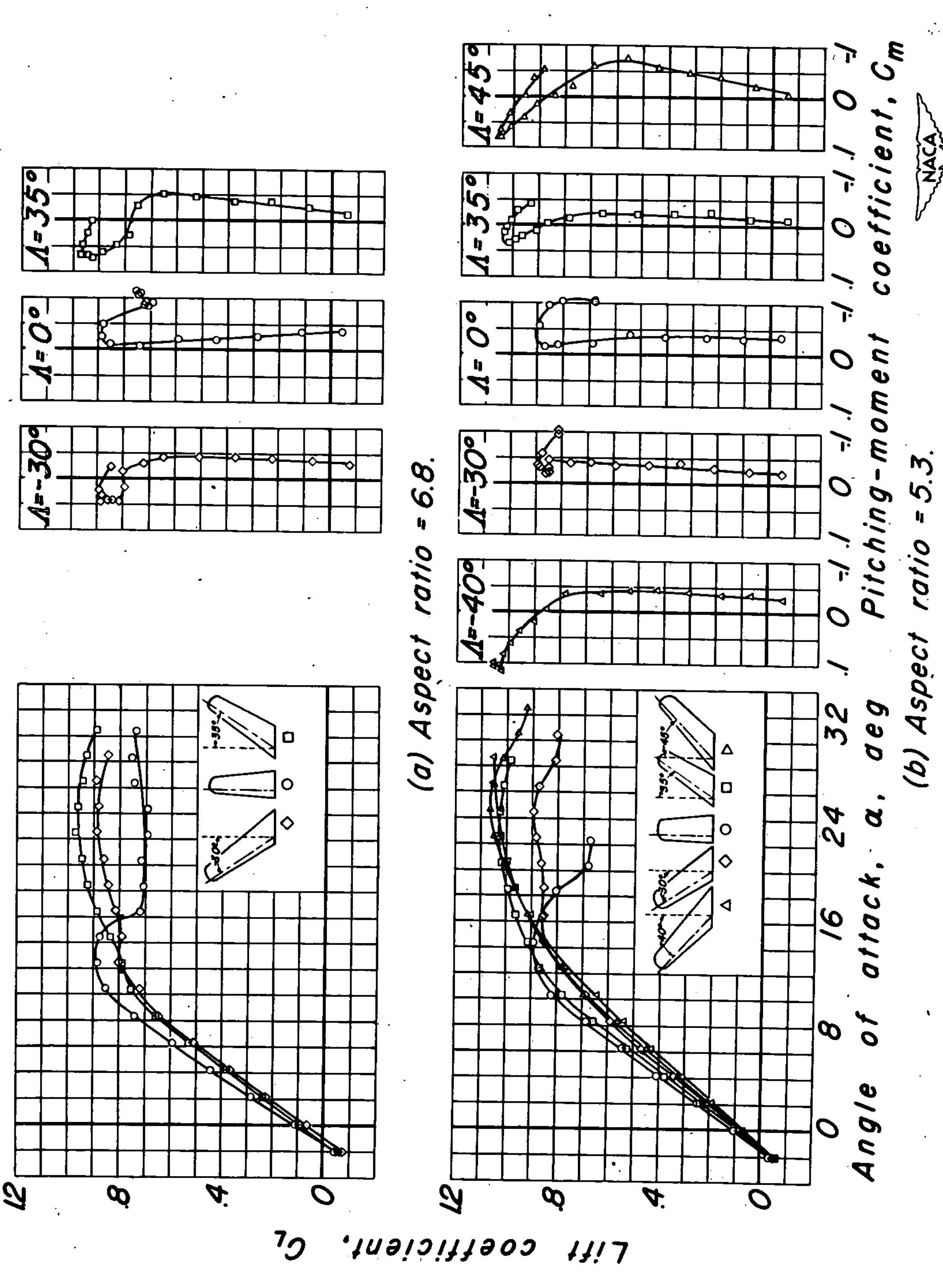

Figure 4.- Effect of sweep on the lift and pitching-moment characteristics of wings.

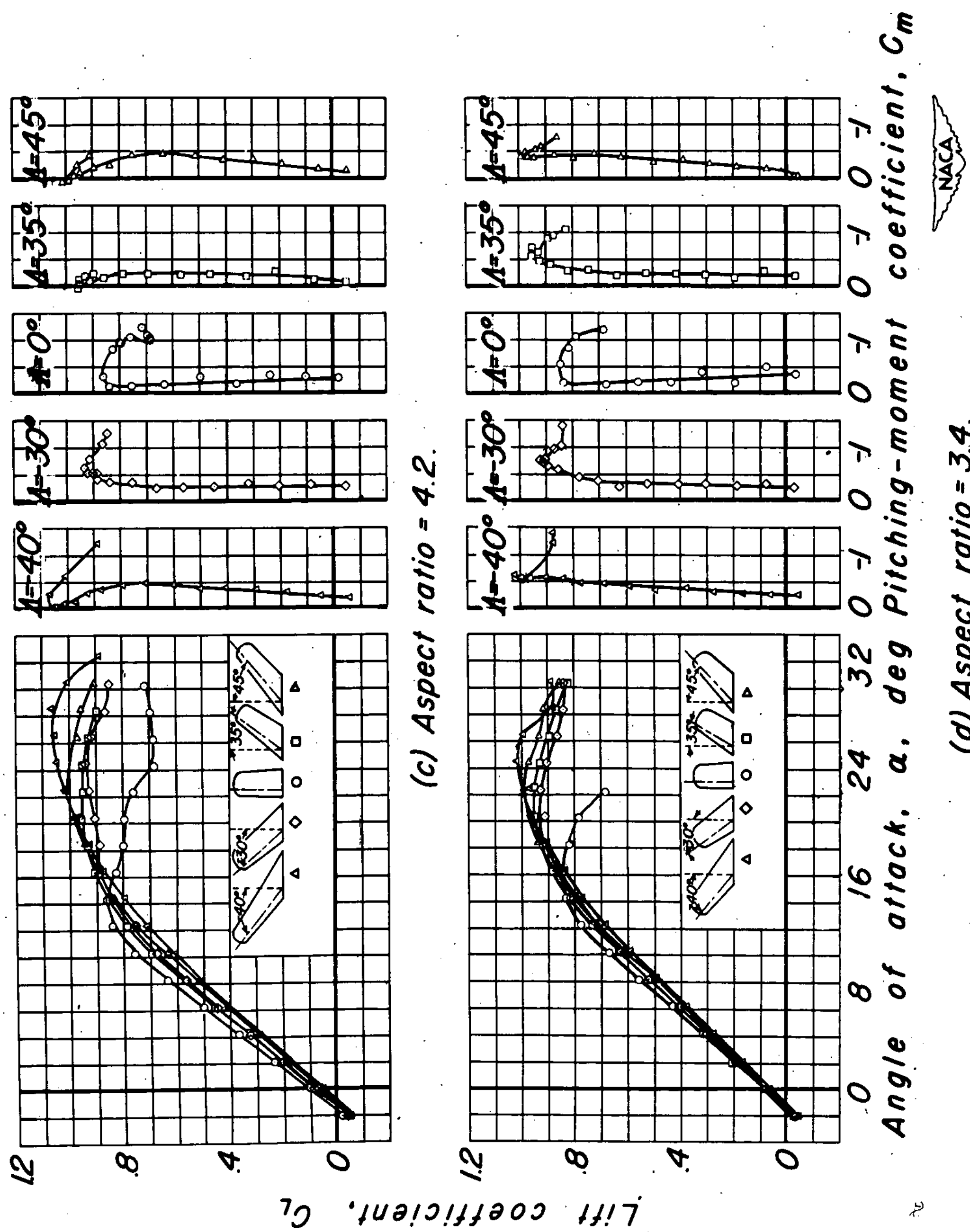

(c) Aspect ratio = 4.2.

(d) Aspect ratio = 3.4.

Figure 4.- Continued.

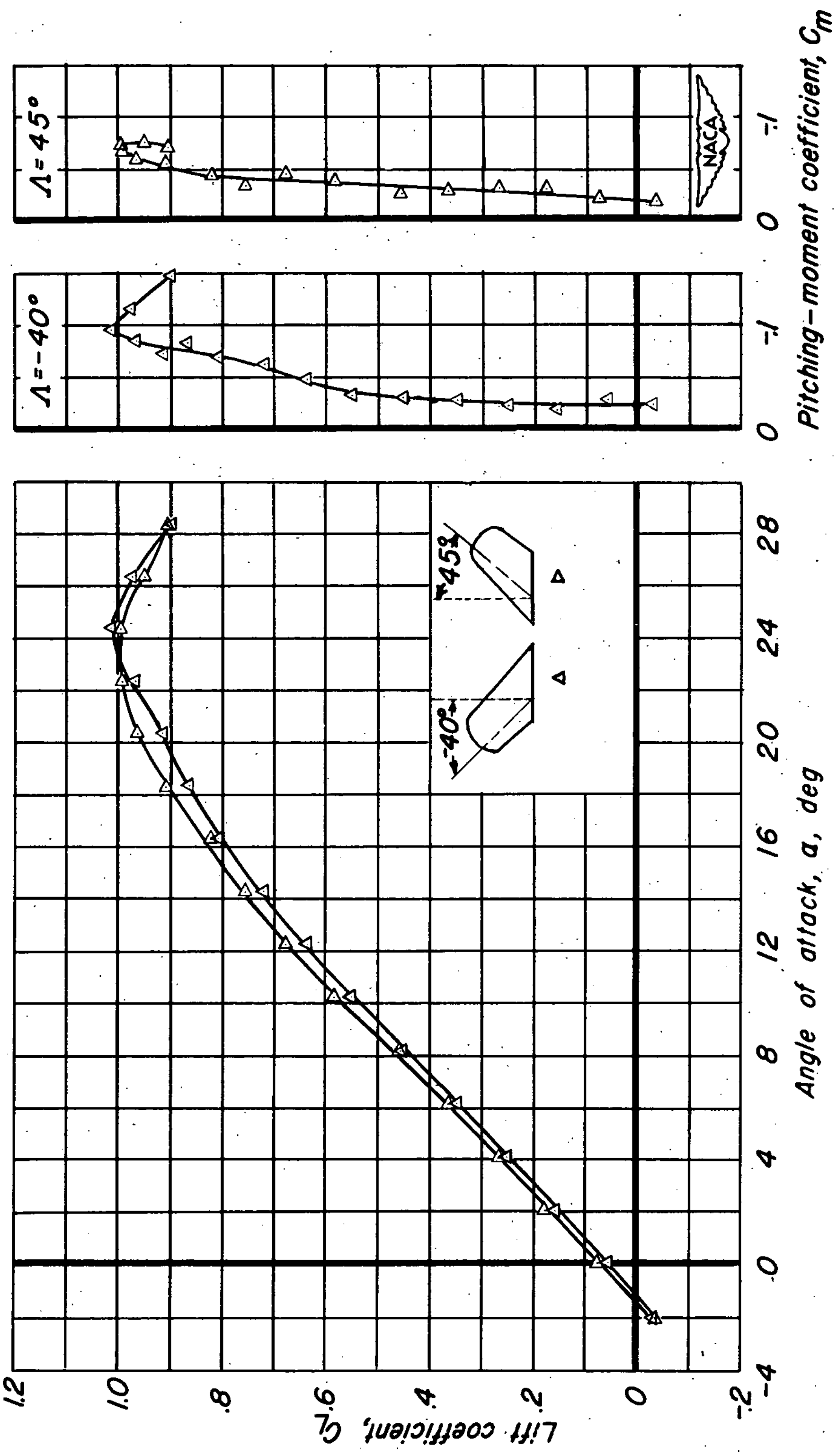

(e) Aspect ratio = 2.8.

Figure 4.- Concluded.

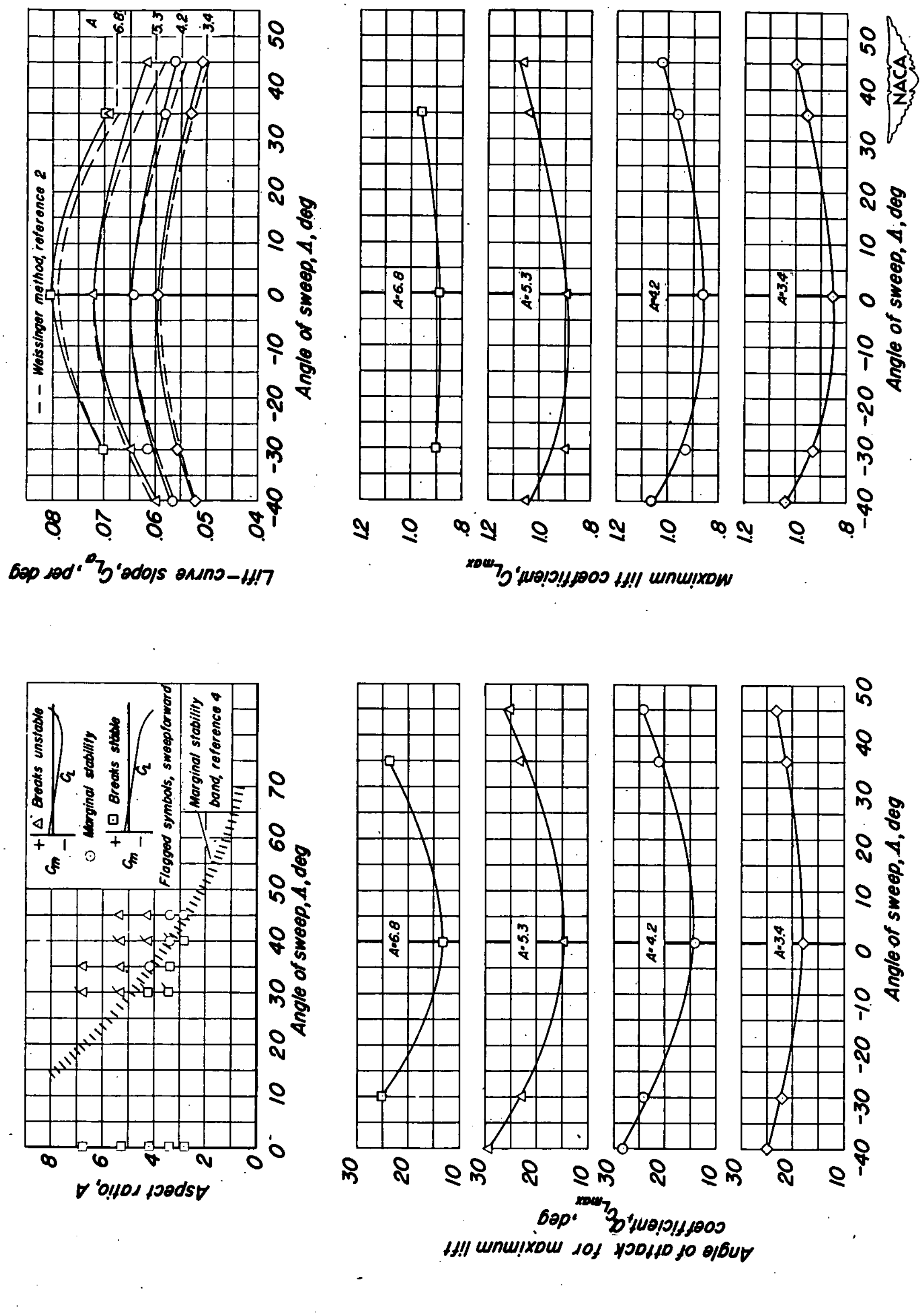

Figure 5.- Effect of sweep and aspect-ratio variations on the aerodynamic parameters of the wings.

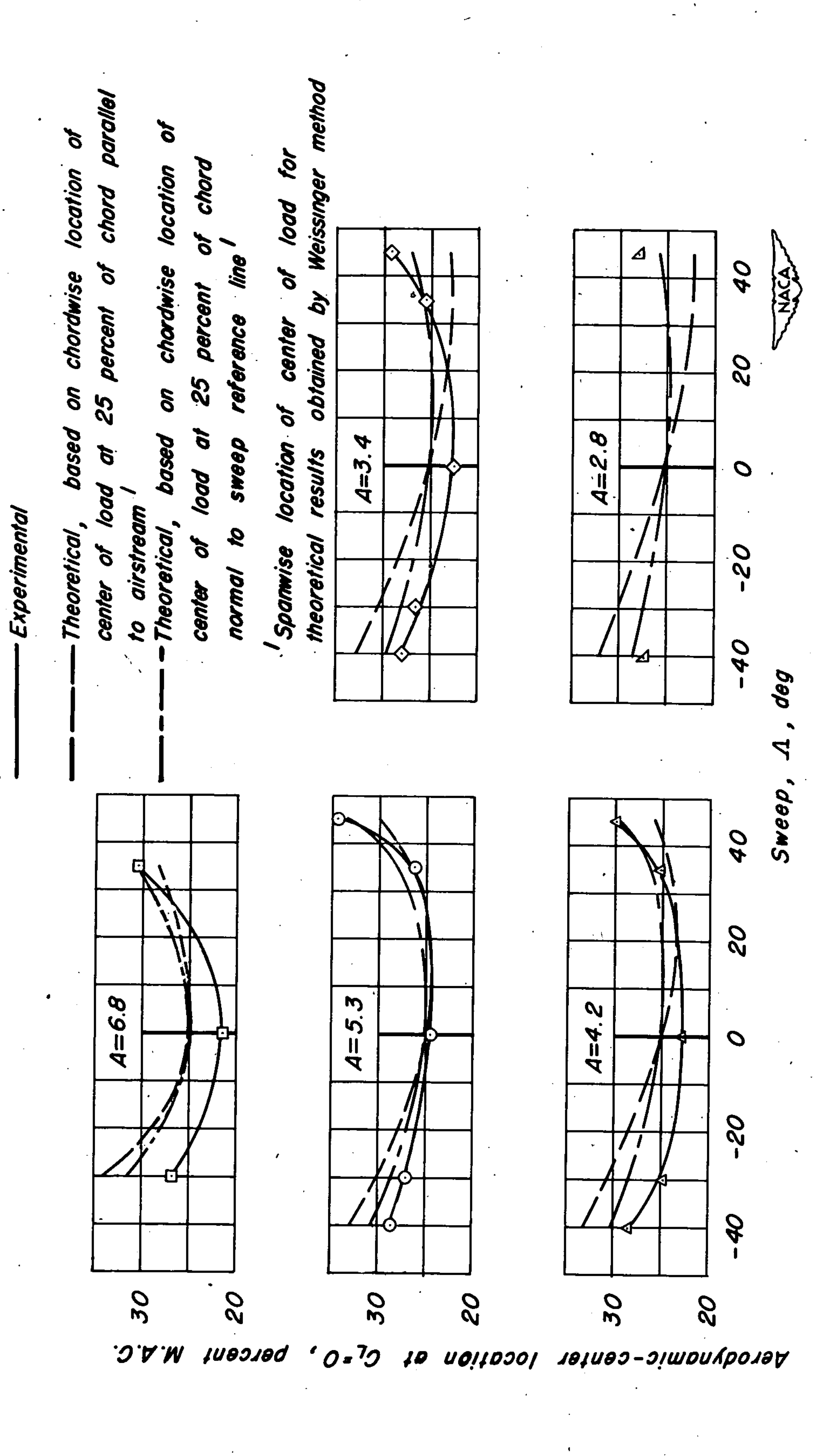

Figure 6.- Effect of sweep on the aerodynamic-center location of wings of several aspect ratios.

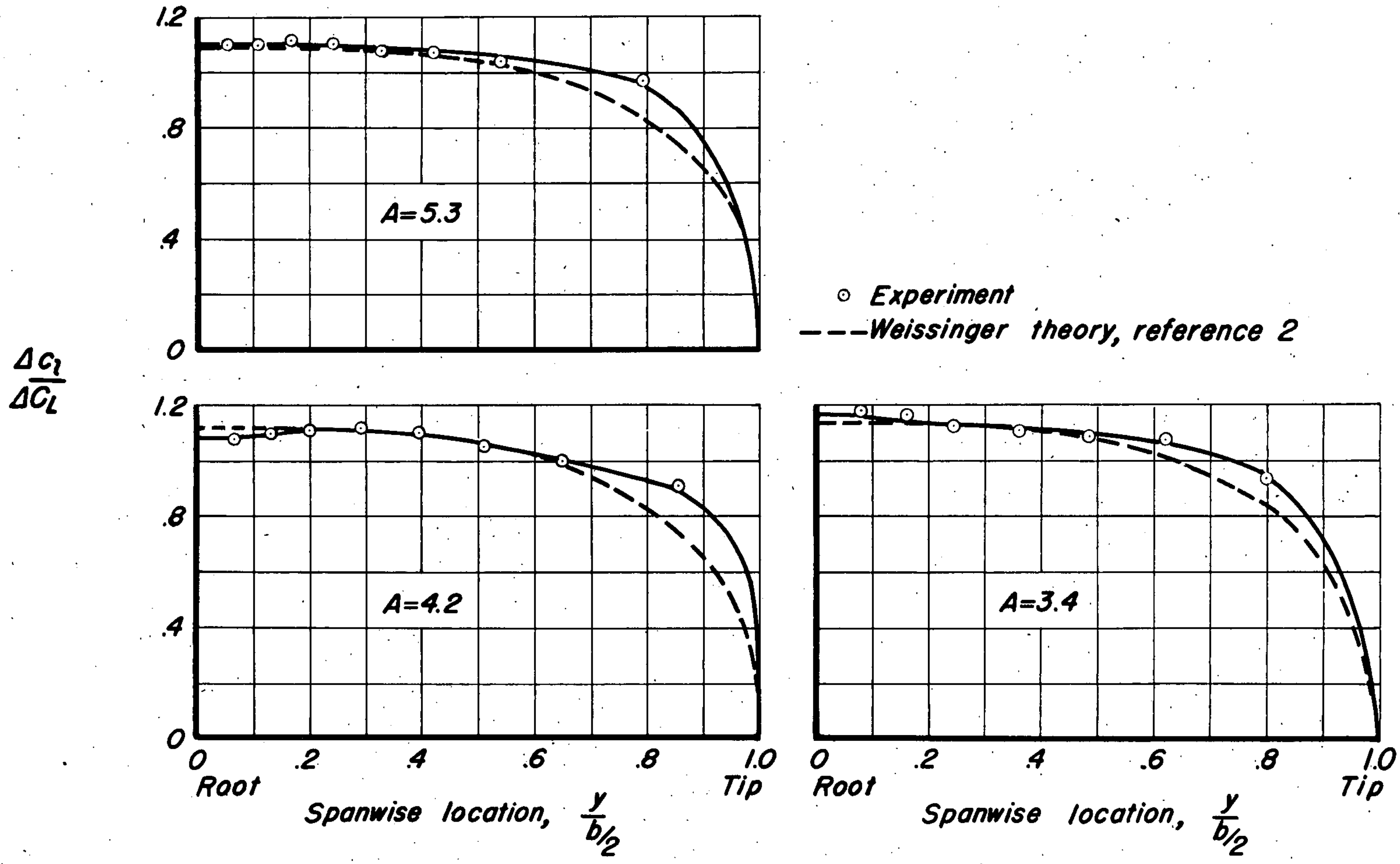

(a) $\Lambda = -40°$.

Figure 7.- Spanwise distribution of $\Delta c_l/\Delta C_L$ for wings of several aspect ratios.

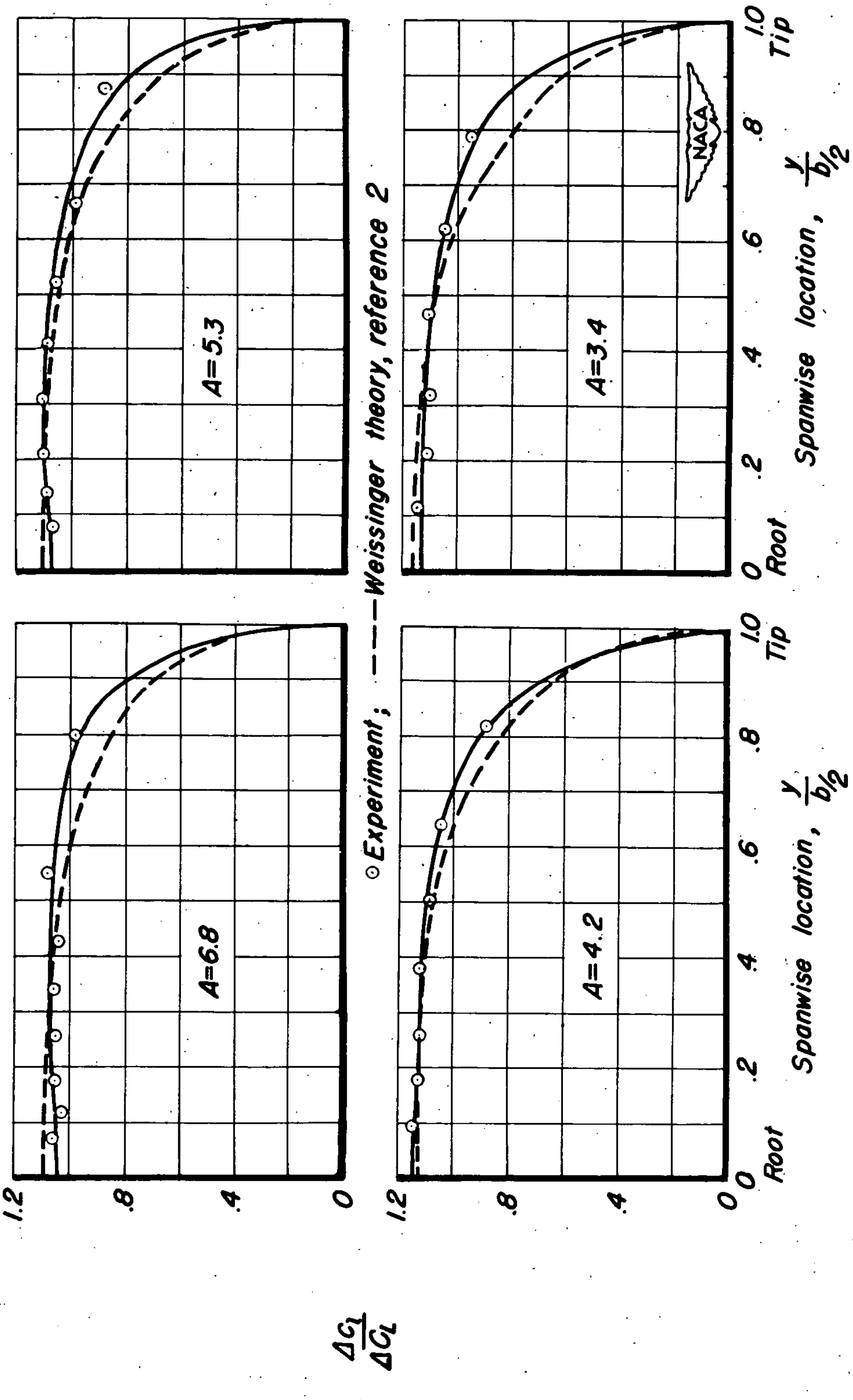

(b) $\Lambda = -30°$.

Figure 7.- Continued.

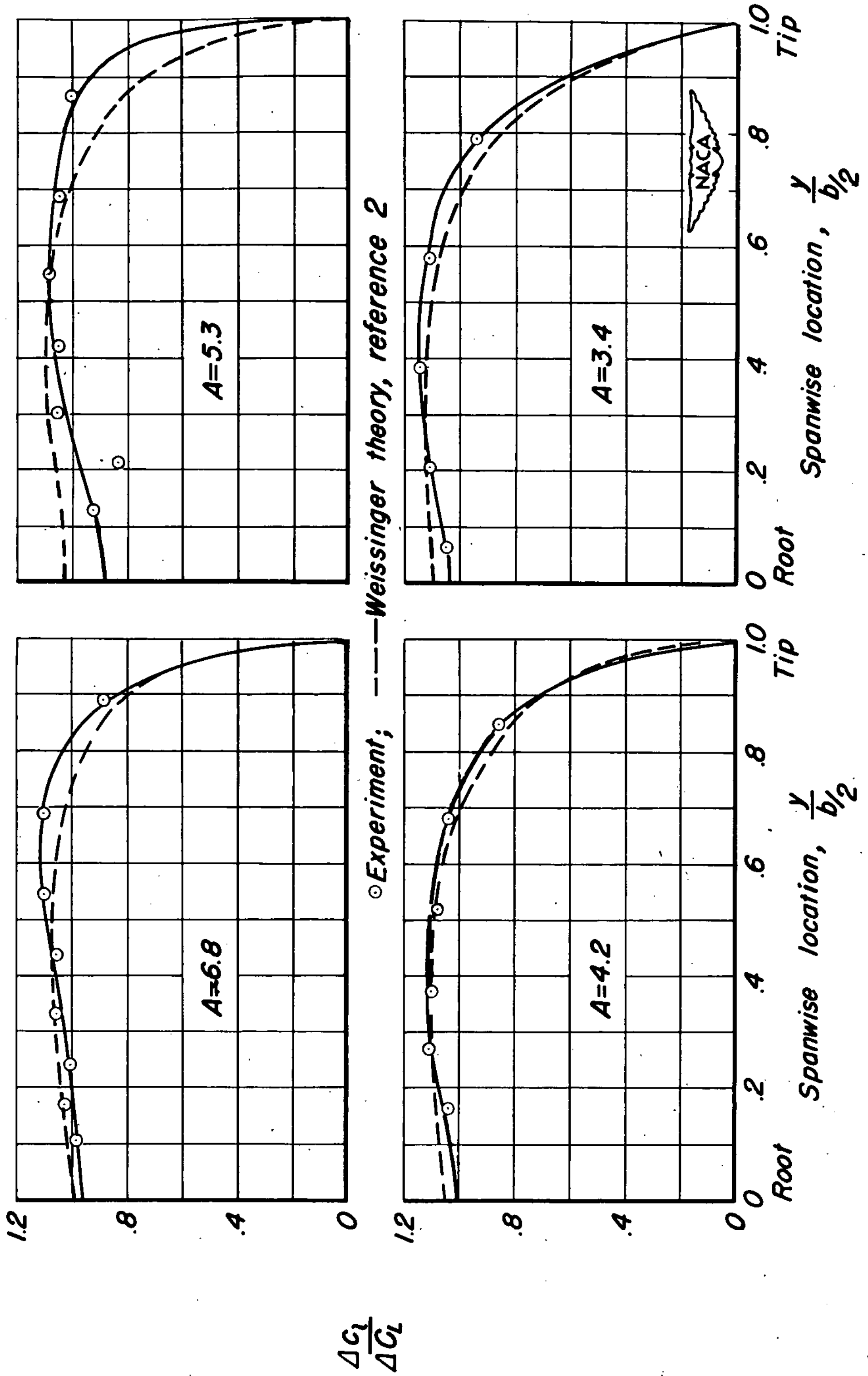

(c) Λ = 0°.

Figure 7.- Continued.

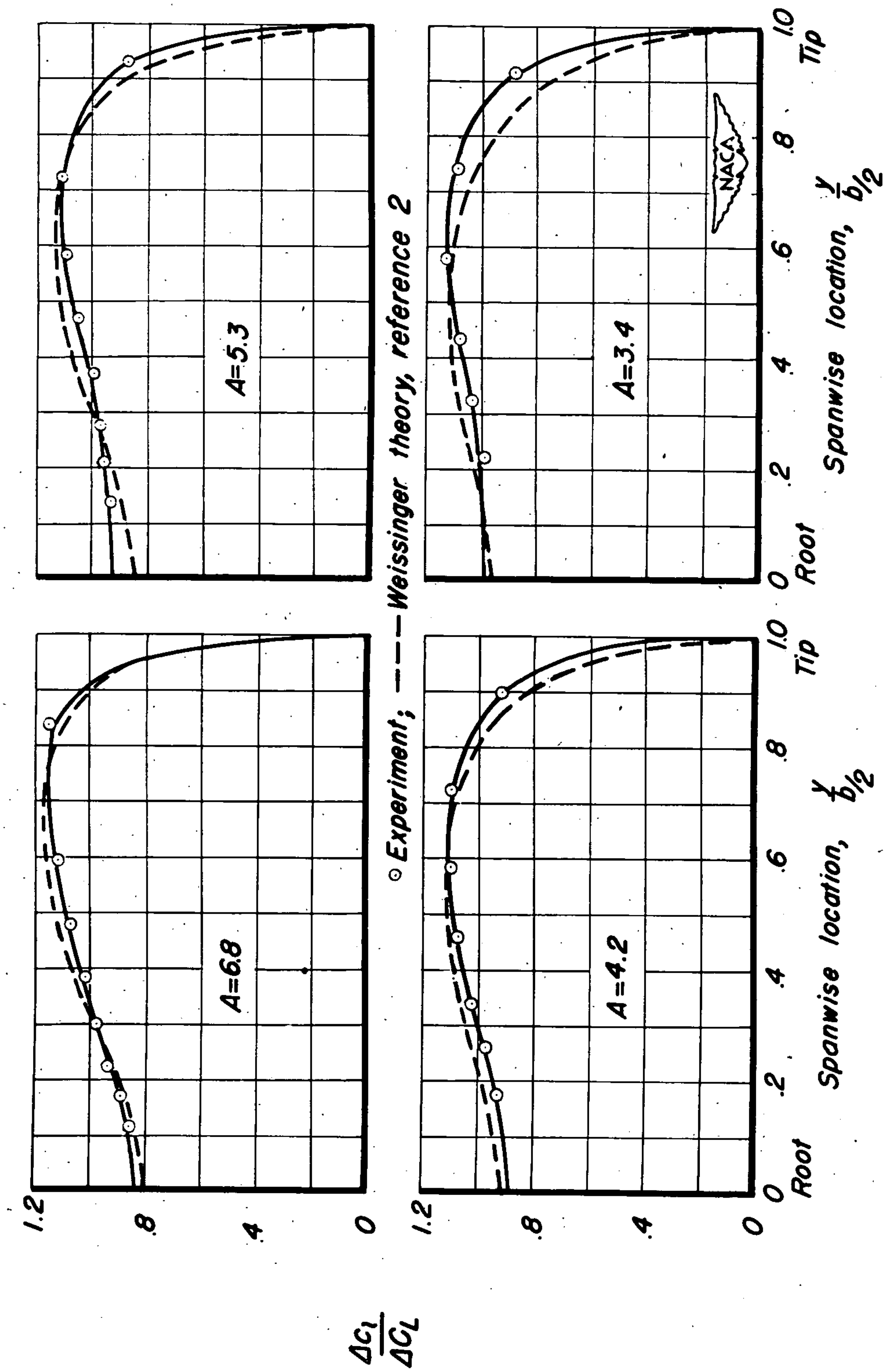

(d) $\Lambda = 35°$.

Figure 7.- Continued.

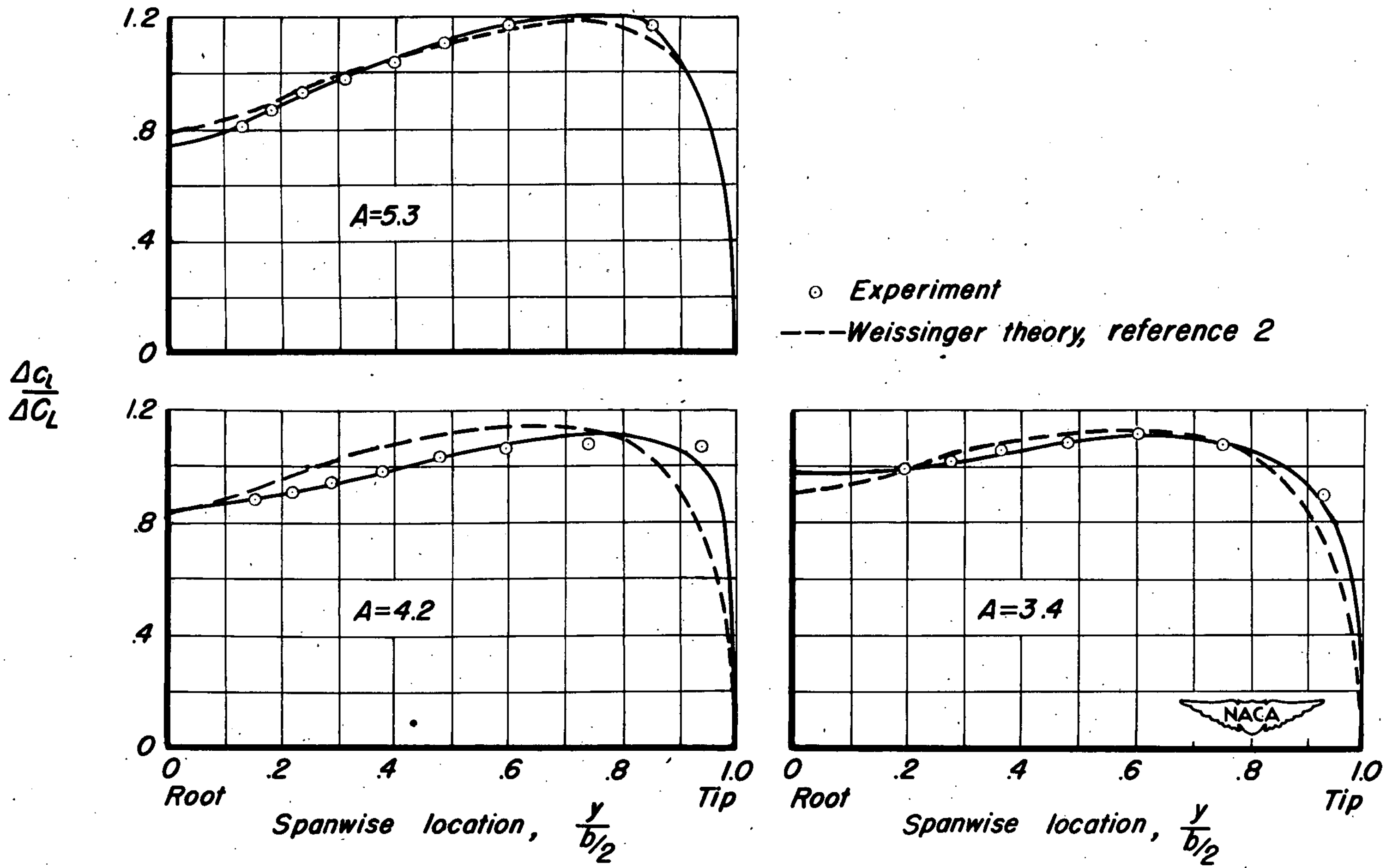

(e) Λ = 45°

Figure 7.- Concluded.

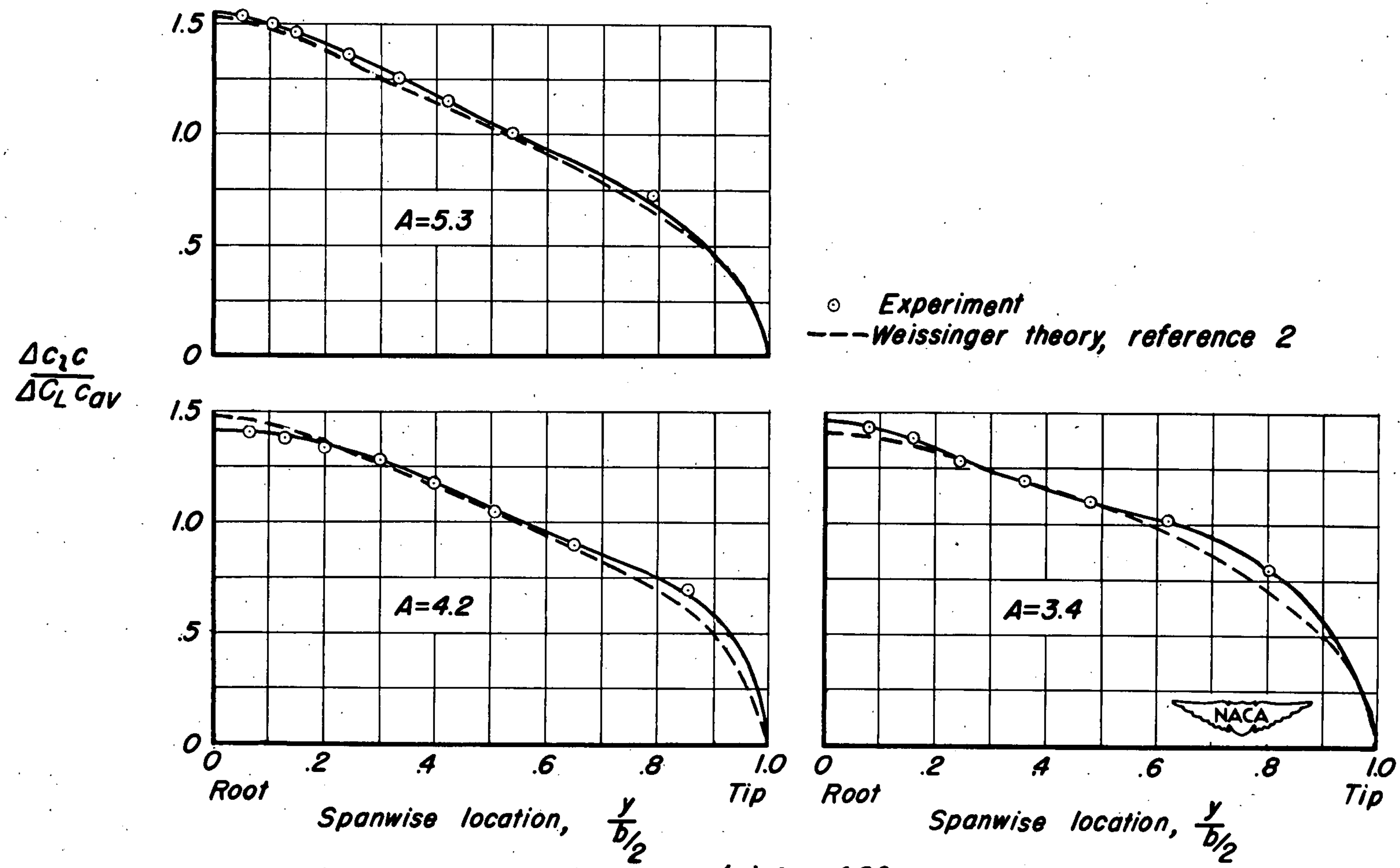

(a) $\Lambda = -40°$.

Figure 8.- Spanwise distribution of $\Delta c_l c/\Delta C_L c_{av}$ for wings of several aspect ratios.

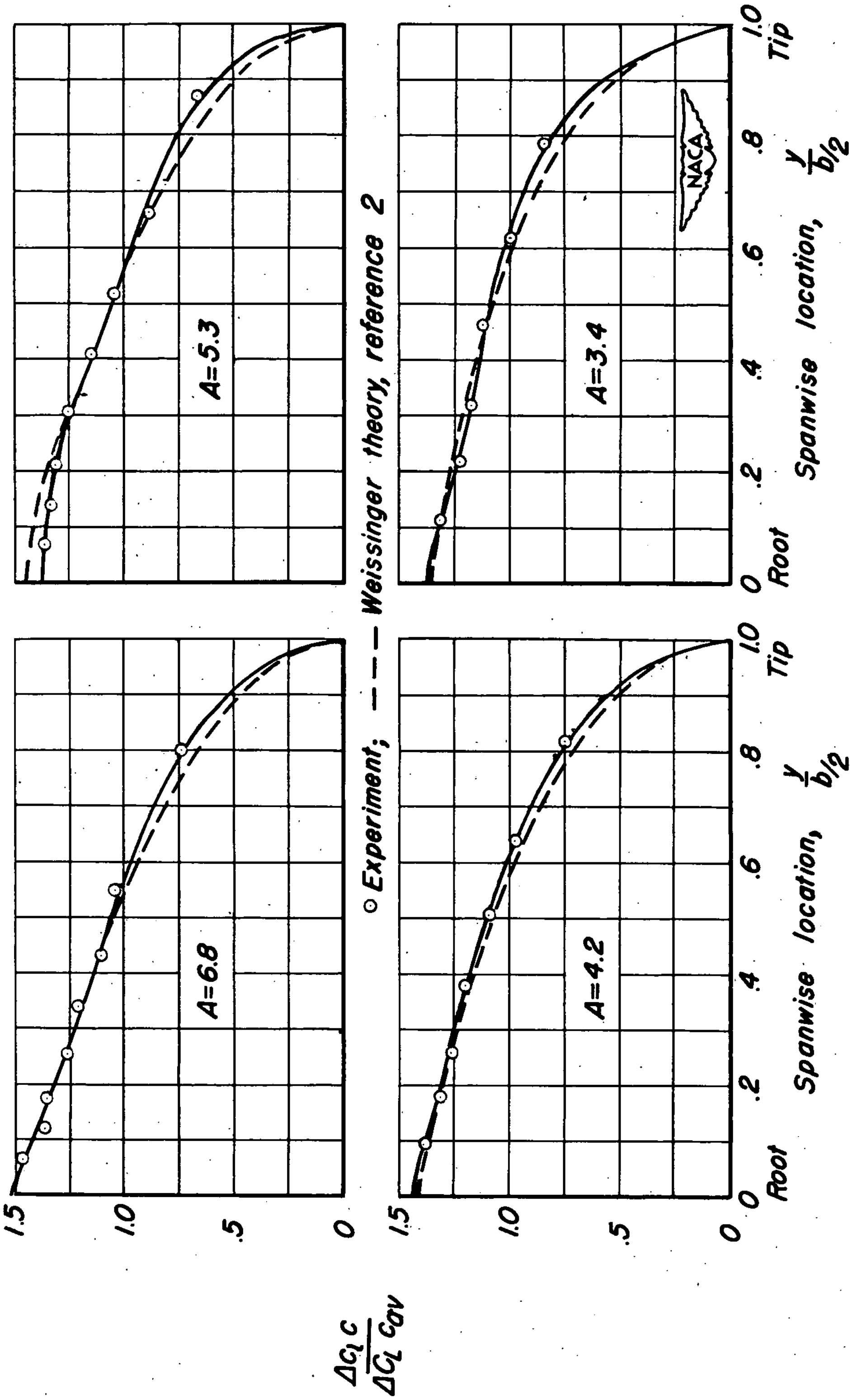

(b) $\Lambda=-30°$.

Figure 8.- Continued.

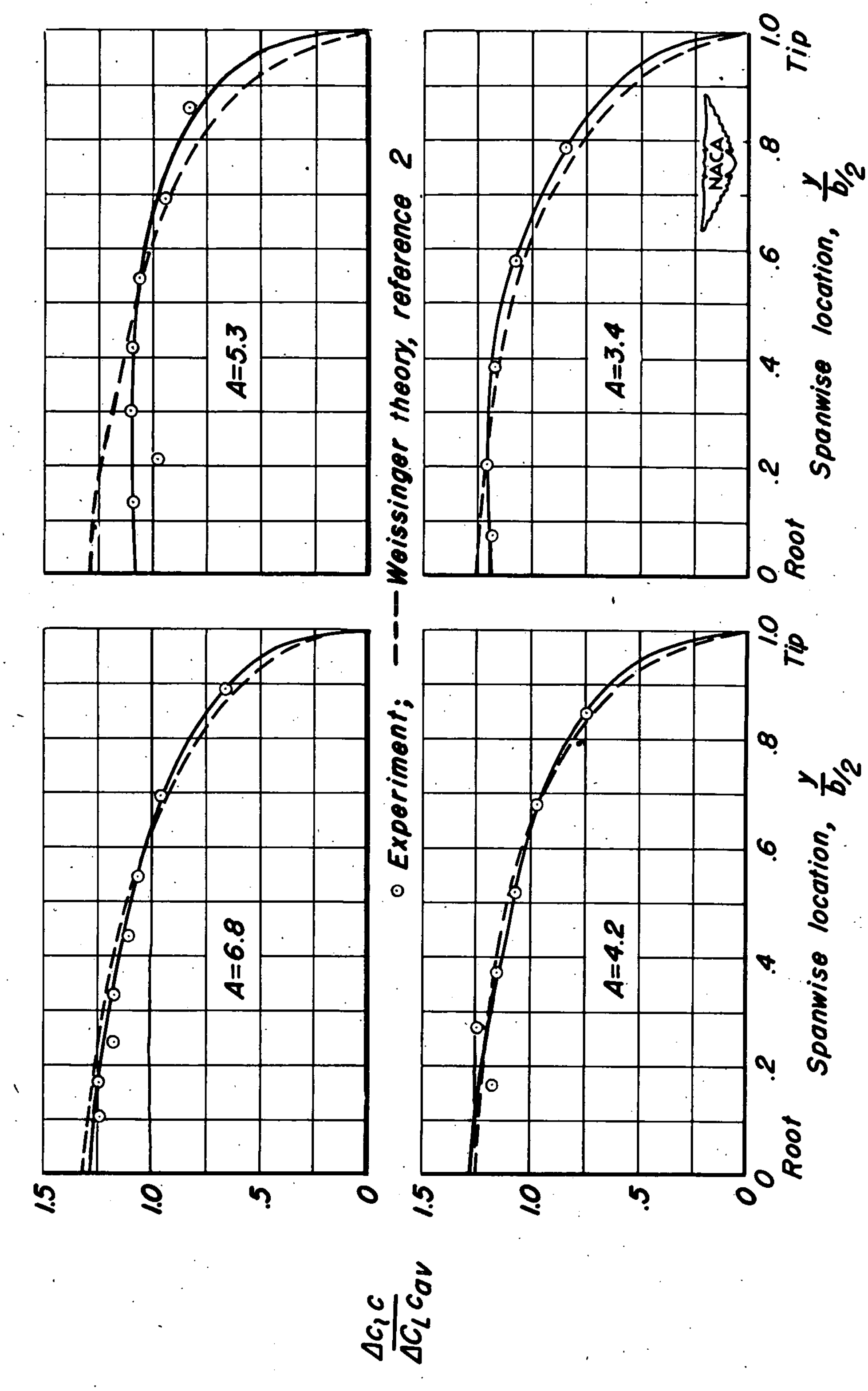

(c) $\Lambda = 0°$.

Figure 8.- Continued.

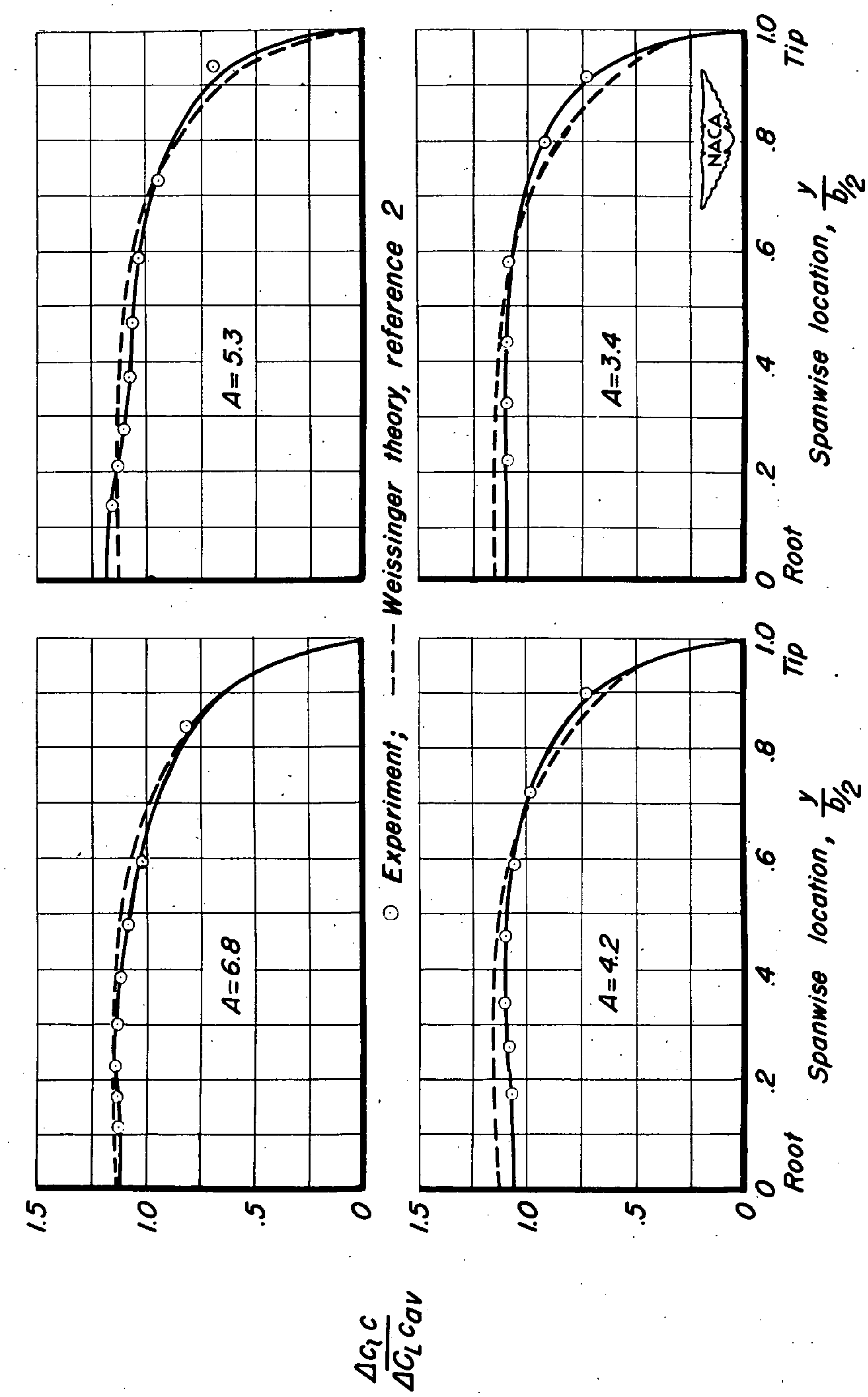

(d) $\Lambda = 35°$.

Figure 8.- Continued.

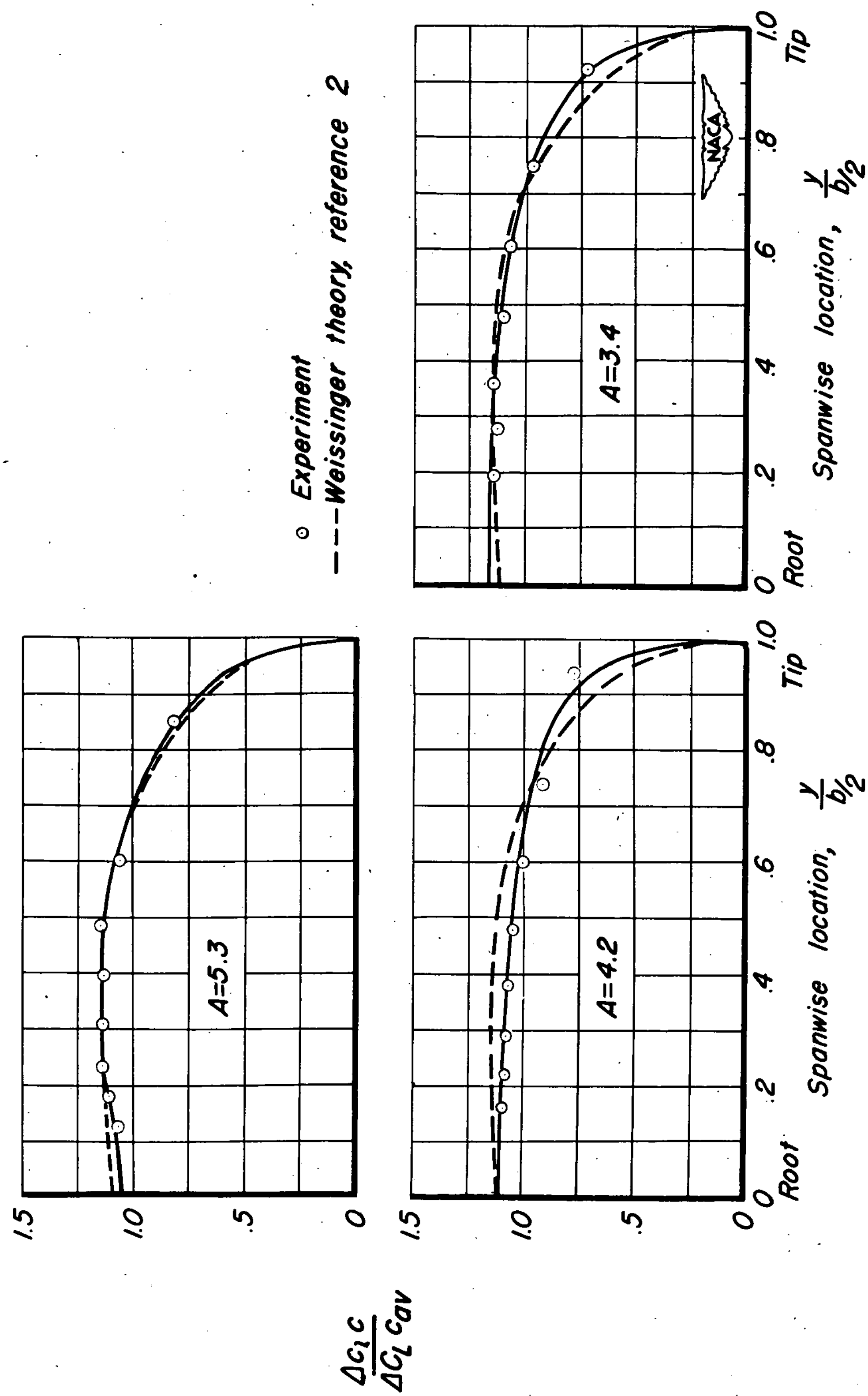

(e) $\Lambda = 45°$.

Figure 8.- Concluded.

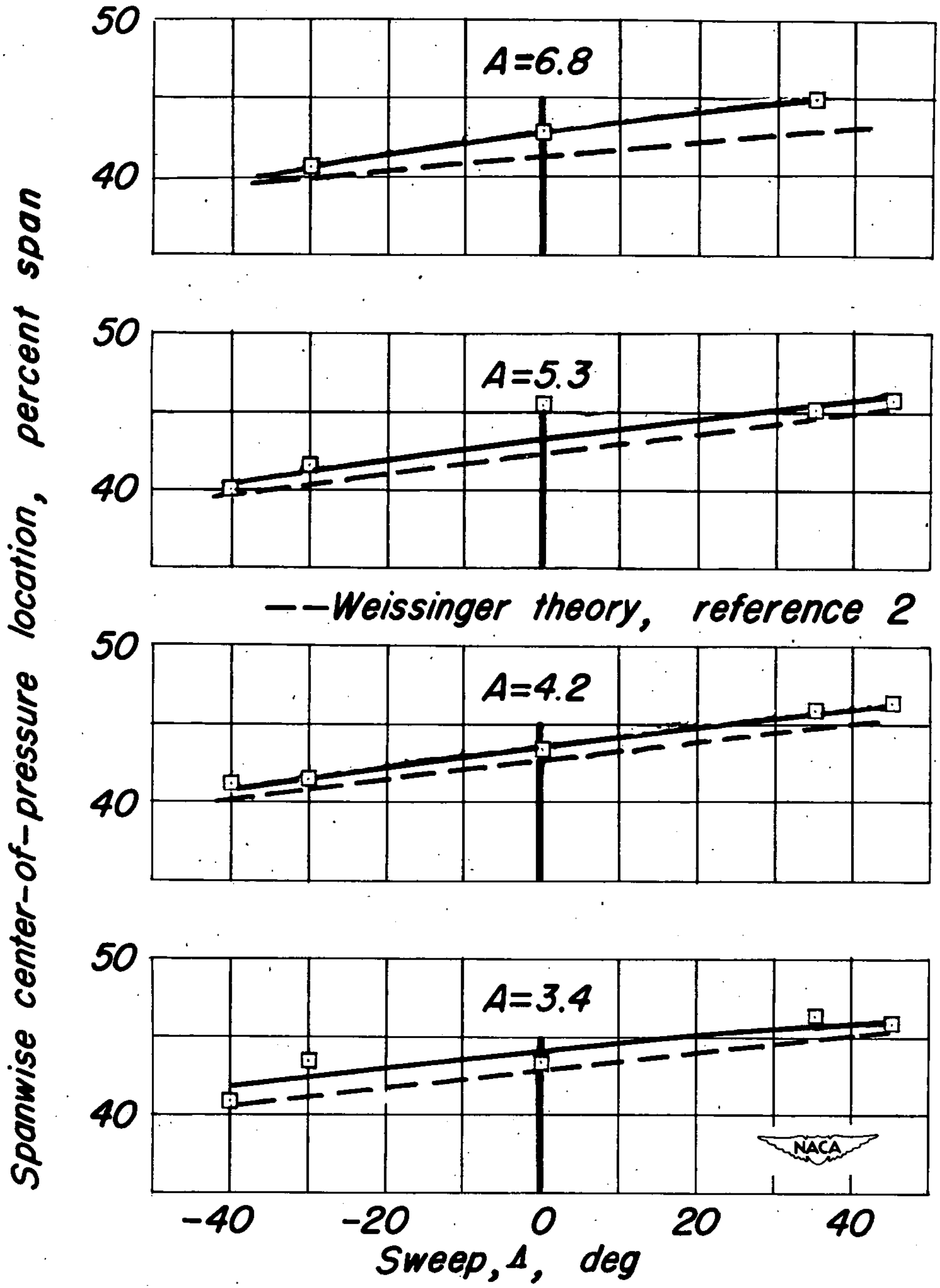

Figure 9.– Effect of sweep on the spanwise center-of-pressure location for wings of several aspect ratios.